Torque Vectoring and Rear-Wheel-Steering Control for Vehicle's Uncertain Slips on Soft and Slope Terrain Using Sliding Mode Algorithm

Zhongchao Liang, Jing Zhao, Zhen Dong, Yongfu Wang, and Zhengtao Ding, *Senior Member, IEEE*

***Abstract*—Off-road vehicles always experience serious uncertain longitudinal and lateral slips when running on soft and slope terrains, and some parameters of the vehicles, such as the cornering stiffness and the slip of wheels, are always not constants. In this paper, control strategies for the torque of each wheel and the rear-wheel-steering angle are proposed to maintain a stable velocity and approach an ideal reference model for the off-road vehicle by using second-order sliding mode (SOSM) techniques. An observer is constructed to estimate the actual sideslip angle of the vehicle with the consideration of uncertainties and disturbances of the system. Then, with conditions of bounded uncertainties and disturbances, composite super-twisting (ST) controllers combined with a velocity controller are designed to generate the total torque, the differential torque, and the rear-wheel-steering angle. On this basis, the proposed controllers have been verified to lead good robustness for maintaining the stable velocity and approaching the ideal reference model by using an optimal torque allocation controller at a lower layer. In comparison with conventional yaw moment controllers without the rear-wheel-steering control, the proposed controllers are shown to be more effective.**

***Index Terms*—Torque vectoring, rear-wheel-steering control, direct yaw moment control, sliding mode, uncertain slips, soft terrain.**

I. Introduction

OFF-ROAD vehicles are considered to drive on off-paved surfaces, such as sandy beach, desert, forest and even planetary surface. Meanwhile, when running under off-road environments where deformable and rough terrains exist, dynamical characteristics of vehicles are complex [1], [2]. As a result, wheels show easily slips and traction losses on the loose soil [3]. Moreover, some parameters of the vehicle on a slope terrain, including the cornering stiffness and the slip of wheels, are always not constants due to the variation of the normal force of each wheel. For these reasons, drivers will face more difficulties when driving the vehicle under the off-road environments than on smooth and hard-paved roads.

Some researchers have focused on precisely modeling the interaction of wheel with soft soil, which is a key part for evaluating the performance of vehicles [4], [5]. Semi-empirical models basing on Bekker's normal stress [6] and Janosi's shear stress equations [7] are mostly used for studying soil properties during interaction with wheels. Then, the relationship among the slip, longitudinal traction, lateral force, vertical load and torque of a single wheel can be derived [8]. On this basis, the wheel-soil model and the multibody model can be combined and utilized to describe motion dynamics of vehicles. As long as longitudinal and lateral slips of the wheel are obtained, control algorithms are able to effectively compensate the vehicle slips in order to follow a given path or approach an ideal model [9]. Furthermore, the real-time estimation for terrain parameters can be applied to improve the model accuracy and control the vehicle traversing on deformable terrains [10]. However, as positions of the vehicle on a slope are always varying, the establishment of the wheel-soil model is difficult to determine the terrain force, and there are also some compromise problems between the model accuracy and the calculation efficiency.

From another perspective, the longitudinal and lateral slips of wheels and the variations of parameters can be treated as some unknown disturbances and uncertainties in the vehicle system. Several methods have already been used for the stability control of land (ground) vehicles, and the proportional- integral-differential (PID) is one of the classic control approaches [11], [12]. However, the PID control is hard to achieve high control performances for complicated systems under unknown conditions. Therefore, many approaches have been developed to fix the problems of complex and nonlinear systems under uncertainties and disturbances, such as the sliding mode control (SMC) [13], the model predictive control (MPC) [14], etc. For MPC methods, future states of vehicle dynamics can be predicted over a finite time horizon, and the cost functions are able to be minimized for prediction horizons under

Manuscript received September 28, 2019; revised December 16, 2019; accepted February 10, 2020. Date of publication February 14, 2020; date of current version April 16, 2020. This work was supported in part by the National Natural Science Foundation of China under Grants 51975109, 51605082, and 51775013, in part by the Fundamental Research Funds for the Central Universities under Grant N180304015, and in part by the Opening Project of Guangdong Provincial Key Laboratory of Technique and Equipment for Macromolecular Advanced Manufacturing, South China University of Technology, China, under Grant 2019kfkt06. The review of this article was coordinated by Dr. D. Cao. *(Corresponding author: Jing Zhao.)*

Zhongchao Liang and Yongfu Wang are with the School of Mechanical Engineering and Automation, Northeastern University, Shenyang 110819, China (e-mail: liangzc@me.neu.edu.cn; yfwang@mail.neu.edu.cn).

Jing Zhao is with the School of Mechanical Engineering and Automation, Northeastern University, Shenyang 110819, China, and also with the Guangdong Provincial Key Laboratory of Technique and Equipment for Macromolecular Advanced Manufacturing, South China University of Technology, Guangzhou 510641, China (e-mail: zhaoj@mail.neu.edu.cn).

Zhen Dong and Zhengtao Ding are with the Department of the Electrical and Electronic Engineering, University of Manchester, Manchester M13 9PL, U.K. (e-mail: zhen.dong@manchester.ac.uk; zhengtao.ding@manchester.ac.uk).

Digital Object Identifier 10.1109/TVT.2020.2974107

0018-9545 © 2020 IEEE. Personal use is permitted, but republication/redistribution requires IEEE permission.
See https://www.ieee.org/publications/rights/index.html for more information.

Authorized licensed use limited to: Seoul National University. Downloaded on August 26,2024 at 05:27:08 UTC from IEEE Xplore. Restrictions apply.

a set of operation constraints [15]. Therefore, the MPC approaches have been widely studied, and applied in the electronic stability control (ESC) [16], the adaptive cruise control (ACC) [17], the path following [18], and the energy management [19] for vehicle systems. However, the MPC-based approaches may cause some computational burdens in finding optimal solutions, and induce accuracy losses when using simplified models in some critical situations [20]. As an effective tool to suppress disturbances for complex systems, the SMC algorithm is proposed to be used in this study due to its satisfactory control performances for nonlinear systems and unknown disturbances.

It is well known that SMC is a strong robust technique for a variety of nonlinear applications with uncertainties and disturbances. The superior feature of the SMC methods over other robust control ones is its complete compensation of matched disturbances when the system is on the sliding surface [21]. Due to discontinuous sign functions used for the controllers, the conventional first-order SMC methods may exhibit large chattering in actuators. In order to attenuate chattering and enhance control performances, many approaches have been extensively developed, such as disturbance- observer-based control (DOBC) methods for reducing unknown parts of systems [22], and higher-order SMC (HOSMC) methods for conducting continuous controllers which further include second-order sliding-mode (SOSM) control methods [23] and arbitrary order SMC methods [24]. DOBC algorithms could reduce problems of the heavy chattering phenomenon, but need to estimate disturbances in the system with more assumptions with respect to unknown items [25]. Arbitrary order SMC approaches have advantages to achieve chattering free for the controlled system, but would bring more complexities for the controllers [23]. In comparison, the SOSM approaches are able to effectively reduce chattering with high control performances in practices, and easy to implement [26], [27].

Thus, SOSM methods have been widely used in real applications, such as the direct yaw moment control and the four-wheel-steering (4WS) control for improving stability performances of vehicles. To four-wheel independently driven (4WID) electric vehicles (EVs), the SOSM controllers were designed to generate the yaw moment to track ideal reference models [13], [28]. To 4WS vehicles, the SMC approaches were applied to provide high stability performances and low sensitivities to uncertain conditions of the velocity, road condition, and roll axis inclination [29], [30].

Motivated by above discussions, in this paper, the unknown longitudinal and lateral slips and the uncertain vehicle parameters are considered, and the SOSM-based super-twisting (ST) control strategies are presented to maintain a constant velocity and approach an ideal reference model for the off-road vehicle running on the soft and slope terrain. The main contributions of this study are stated as follows.

1) A nonlinear vehicle system is established with the consideration of uncertain parameters and slips, and an observer is constructed to estimate the actual sideslip angle of the vehicle by measuring the yaw rate and the lateral acceleration.

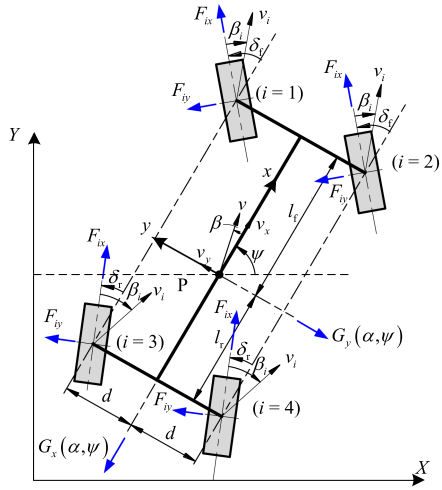

Fig. 1. Dynamic model for off-road vehicle.

2) To cruise at a stable velocity for the off-road vehicle, a velocity controller is designed by using ST algorithms. On this basis, the velocity controller is proposed to generate total torques for four wheels and impose longitudinal tractions on the vehicle body.
3) Composite controllers, including a differential torque controller and a rear-wheel-steering controller, are designed to track an ideal reference model. Then, the composite controllers combined with the velocity controller at a upper layer and a optimal torque allocation controller at a lower layer are proposed to exert the torque on each wheel and generate the steering angle for rear wheels.

The remainder of this paper is organized as the following. The vehicle dynamic model is established in Section II. The sideslip angle observer construction and the controllers design are presented in Section III. In Section IV, simulations are conducted to verify the proposed controllers. Finally, the conclusions of this paper are drawn in Section V.

II. Vehicle Dynamics and Problem Formulation

A. Vehicle Dynamic Model

A vehicle dynamic model is shown in Fig. 1, and the subscript *i* denotes the wheel ID. Descriptions for main parameters of the vehicle are shown in Table I.

The motion along *x*-axis can be expressed as

$$m\left(\dot{v}_x - v_y\gamma\right) + mg\ \sin\alpha_{\rm g} = F_{{\rm fa}x}\cos\delta_{\rm f} + F_{{\rm ra}x}\cos\delta_{\rm r} - F_{{\rm fa}y}\sin\delta_{\rm f} - F_{{\rm ra}y}\sin\delta_{\rm r} \tag{1}$$

where $F_{{\rm fa}x} = F_{1x} + F_{2x}$, $F_{{\rm ra}x} = F_{3x} + F_{4x}$, $F_{{\rm fa}y} = F_{1y} + F_{2y}$, and $F_{{\rm ra}y} = F_{3y} + F_{3y}$.

The motion along *y*-axis can be expressed as

$$m\left(\dot{v}_y + v_x\gamma\right) + mg\ \sin\ \alpha_{\rm b} = F_{{\rm fa}x}\sin\delta_{\rm f} + F_{{\rm ra}x}\sin\delta_{\rm r} + F_{{\rm fa}y}\cos\delta_{\rm f} + F_{{\rm ra}y}\cos\delta_{\rm r} \tag{2}$$

Authorized licensed use limited to: Seoul National University. Downloaded on August 26,2024 at 05:27:08 UTC from IEEE Xplore. Restrictions apply.

TABLE I
VARIABLES FOR VEHICLE MODEL

Symbol	Description
m	Vehicle mass
l_{f}	Distance from center of gravity (CG) to front axle
l_{r}	Distance from CG to rear axle
d	Distance from CG to left/right wheel
i	Wheel ID, and i = 1, 2, 3, 4
F_{ix}/ F_{iy}	Longitudinal/lateral force of wheel i
F_{iz}	Vertical load of wheel i
I_Z	Yaw moment of inertia of vehicle
$\delta_{\mathrm{f}}/\delta_{\mathrm{r}}$	Steering angle of front/rear wheels
g	Gravity acceleration
ψ	Posture angle of vehicle on slope
γ	Yaw rate of vehicle
β	Sideslip angle of vehicle
β_i	Sideslip angle of wheel i
v	Total velocity at CG
v_x/v_y	Longitudinal/lateral velocity at CG
v_i	Velocity of wheel i
a_y	Lateral acceleration of vehicle
α	Slope angle of terrain
α_{g}	Grade angle of vehicle on slope terrain
α_{b}	Bank angle of vehicle on slope terrain

Furthermore, the yaw motion can be expressed as

$$\begin{aligned} I_Z\dot{\gamma} = {} & dF_{\mathrm{fb}x}\cos\delta_{\mathrm{f}} + l_{\mathrm{f}}F_{\mathrm{fa}x}\sin\delta_{\mathrm{f}} \\ & + dF_{\mathrm{rb}x}\cos\delta_{\mathrm{r}} - l_{\mathrm{r}}F_{\mathrm{ra}x}\sin\delta_{\mathrm{r}} \\ & - dF_{\mathrm{fb}y}\sin\delta_{\mathrm{f}} + l_{\mathrm{f}}F_{\mathrm{fa}y}\cos\delta_{\mathrm{f}} \\ & - dF_{\mathrm{rb}y}\sin\delta_{\mathrm{r}} - l_{\mathrm{r}}F_{\mathrm{ra}y}\cos\delta_{\mathrm{r}} \end{aligned} \tag{3}$$

where $F_{\mathrm{fb}x} = F_{2x} - F_{1x}$, $F_{\mathrm{rb}x} = F_{4x} - F_{3x}$, and $F_{\mathrm{fb}y} = F_{2y} - F_{1y}$ and $F_{\mathrm{rb}y} = F_{4y} - F_{3y}$.

Additionally, the grade and bank angles have the following relationships with the yaw angle of the vehicle and the slope angle of the terrain

$$\begin{cases} \sin\alpha_{\mathbf{g}} = \sin\alpha\sin\psi \\ \sin\alpha_{\mathbf{b}} = \sin\alpha\cos\psi \end{cases} \tag{4}$$

B. Problem Formulation

1) Uncertain Longitudinal Slip: According to Wong-Reece pressure distribution model when the vehicle moving on soft terrains, the longitudinal traction force and the driving torque of a single wheel have the following relationships [31], [32]

$$\begin{cases} F_{iz} = bR\int_{\theta_{2i}}^{\theta_{i1}} \left(\sigma_i(\theta)\cos\theta + \tau_i(\theta)\sin\theta\right)\mathrm{d}\theta \\ F_{ix} = bR\int_{\theta_{i2}}^{\theta_{i1}} \left(\tau_i(\theta)\cos\theta - \sigma_i(\theta)\sin\theta\right)\mathrm{d}\theta \\ T_{si} = bR^2\int_{\theta_{i2}}^{\theta_{i1}} \tau_i(\theta)\,\mathrm{d}\theta \end{cases} \tag{5}$$

where b, R σ_{i}, τ_{i}, θ_{i1} and θ_{i2} are the width, radius, normal pressure, shear stress, entering angle and exit angle of wheel i, respectively; T_{si} is the net torque imposed on wheel i.

However, the wheel model of (5) is so complex to implement on vehicle models. As a result, this model can be simplified using a fitting function basing on experimental data as follows [33]

$$F_{ix} = T_{is}/R - F_{iz}\left(a_s s_i + b_s\right) \tag{6}$$

where s_i is the slip ratio of wheel i; a_s and b_s are fitting coefficients.

By introducing the driving efficiency of motors η_{i}, (6) can be rewritten as

$$F_{xi} = \left(T_i - \Delta T_i\right)/R \tag{7}$$

where T_i is the torque of motor i; $\Delta T_i = (1-\eta_{\mathrm{i}})T_{\mathrm{i}} + RF_{zi}(a_s s_i + b_s)$; η_{i} is the efficiency from diving motor i to wheel i. T_i, F_{zi}, η_i and s_{i} are assumed to be bounded, and thus there exists a positive constant T_{S} such that $|\Delta T_i| \le T_{\mathrm{S}}$. Furthermore, it is assumed that the tractive force F_{xi} and the toque T_i will stay away from the capacity boundaries of tires and motors.

2) Uncertain Lateral Sideslip: The cornering stiffness of wheels is mostly treated as a constant parameter to facilitate the controller design [34], and the lateral forces of front and rear wheels can be written as

$$\begin{cases} F_{\mathrm{fa}y} = c_{\mathrm{f}}\beta_{\mathrm{f}} \\ F_{\mathrm{ra}y} = c_{\mathrm{r}}\beta_{\mathrm{r}} \end{cases} \tag{8}$$

where β_{f} and β_{r} are the equivalent sideslip angles of front and rear wheels, respectively; c_{f} and c_{r} are the equivalent constants of front-wheel and rear-wheel cornering stiffness, respectively.

With kinematics of the vehicle, the sideslip angles of four wheels can be derived as

$$\beta_{1,2} \approx \beta_{\mathrm{f}} = \delta_{\mathrm{f}} - \beta - \frac{l_{\mathrm{f}}}{v}\gamma, \quad \beta_{3,4} \approx \beta_{\mathrm{r}} = \delta_{\mathrm{r}} - \beta + \frac{l_{\mathrm{r}}}{v}\gamma \tag{9}$$

However, for off-road vehicles on soft and slope terrains, the lateral force of each wheel calculated by a linear model of cornering stiffness may not accurate, and values of the cornering stiffness are dependent on terrain conditions and normal forces on wheels. With the consideration of uncertain lateral sideslips and model nonlinearities, the actual cornering stiffness of wheel i is denoted as c_i, and the lateral force of wheel i can be expressed as

$$F_{iy} = c_i\beta_i \tag{10}$$

For the vehicle running on soft and slope terrains, c_i is not a constant. As a result, c_{f} and c_{r} are, respectively, the nominal constant parts of $c_1 + c_2$ and $c_3 + c_4$. Then, the cornering stiffness of each wheel can be expressed as

$$\begin{cases} c_1 = c_{\mathrm{f}}/2 + \Delta c_1, \quad c_2 = c_{\mathrm{f}}/2 + \Delta c_2, \\ c_3 = c_{\mathrm{r}}/2 + \Delta c_3, \quad c_4 = c_{\mathrm{r}}/2 + \Delta c_4, \end{cases} \tag{11}$$

where Δc_i is the uncertain and nonlinear part of the cornering stiffness of wheel i, and satisfies $|\Delta c_i| \le c_{\mathrm{S}}/2$.

With considerations of the uncertain cornering stiffness, the actual lateral force variables in (1)–(3) can be obtained as

$$\begin{cases} F_{\mathrm{fa}y} = (c_1 + c_2)\,\beta_{\mathrm{f}} = (c_{\mathrm{f}} + \Delta c_1 + \Delta c_2)\,(\delta_{\mathrm{f}} - \beta - l_{\mathrm{f}}\gamma/v) \\ F_{\mathrm{ra}y} = (c_3 + c_4)\,\beta_{\mathrm{r}} = (c_{\mathrm{r}} + \Delta c_3 + \Delta c_4)\,(\delta_{\mathrm{r}} - \beta + l_{\mathrm{r}}\gamma/v) \\ F_{\mathrm{fb}y} = (c_2 - c_1)\,\beta_{\mathrm{f}} = (\Delta c_2 - \Delta c_1)\,(\delta_{\mathrm{f}} - \beta - l_{\mathrm{f}}\gamma/v) \\ F_{\mathrm{rb}y} = (c_4 - c_3)\,\beta_{\mathrm{r}} = (\Delta c_4 - \Delta c_3)\,(\delta_{\mathrm{r}} - \beta + l_{\mathrm{r}}\gamma/v) \end{cases} \tag{12}$$

Authorized licensed use limited to: Seoul National University. Downloaded on August 26,2024 at 05:27:08 UTC from IEEE Xplore. Restrictions apply.

3) Vehicle System: As δ_{f} and δ_{r} are small, the following simplifications are used: $\sin\delta_{\mathrm{f}} \approx \delta_{\mathrm{f}}$, $\sin\delta_{\mathrm{r}} \approx \delta_{\mathrm{r}}$, $\cos\delta_{\mathrm{f}} \approx 1$, $\cos\delta_{\mathrm{r}} \approx 1$. Let the total torque $T_{\mathrm{a}} = T_1 + T_2 + T_3 + T_4$, and the differential torque $T_{\mathrm{b}} = T_2 - T_1 + T_3 - T_4$. By substituting (7) and (12) into (1)–(3), the vehicle system can be obtained when $v > 0$

$$\begin{cases} \dot{v} = F_{v1}(\beta,\gamma,v,\delta_f) + F_{v2}(\beta,\gamma,v,\delta_r) + T_{\mathrm{a}}/(Rm) \\ \qquad - g\sin\alpha(\beta\cos\psi + \sin\psi) + \varepsilon_v \\ \dot{\beta} = A_{11}\beta + A_{12}\gamma + B_1[\delta_{\mathrm{f}} \;\; \delta_{\mathrm{r}} \;\; T_{\mathrm{b}}]^{\mathrm{T}} + E_1(\beta,\gamma,\psi) + \varepsilon_\beta \\ \dot{\gamma} = A_{21}\beta + A_{22}\gamma + B_2[\delta_{\mathrm{f}} \;\; \delta_{\mathrm{r}} \;\; T_{\mathrm{b}}]^{\mathrm{T}} + E_2(\beta,\gamma,\psi,u) + \varepsilon_\gamma \end{cases} \tag{13}$$

where

$$A = \begin{bmatrix} -\frac{c_{\mathrm{f}}+c_{\mathrm{r}}}{mv} & -1 + \frac{c_{\mathrm{r}}l_{\mathrm{r}} - c_{\mathrm{f}}l_{\mathrm{f}}}{mv^2} \\ \frac{l_{\mathrm{r}}c_{\mathrm{r}} - l_{\mathrm{f}}c_{\mathrm{f}}}{I_Z} & -\frac{l_{\mathrm{f}}^2c_{\mathrm{f}} + l_{\mathrm{r}}^2c_{\mathrm{r}}}{vI_Z} \end{bmatrix}, B = \begin{bmatrix} \frac{c_{\mathrm{f}}}{mv} & \frac{c_{\mathrm{r}}}{mv} & 0 \\ \frac{c_{\mathrm{f}}l_{\mathrm{f}}}{I_Z} & -\frac{l_{\mathrm{r}}c_{\mathrm{r}}}{I_Z} & \frac{d}{RI_Z} \end{bmatrix},$$

$$F_{v1} = \frac{c_{\mathrm{f}}}{m}(\beta - \delta_{\mathrm{f}})\left(\delta_{\mathrm{f}} - \beta - \frac{\gamma l_{\mathrm{f}}}{v}\right) - \frac{c_{\mathrm{r}}}{m}\beta\left(\beta - \frac{\gamma l_{\mathrm{r}}}{v}\right),$$

$$F_{v2} = \frac{c_{\mathrm{r}}\delta_{\mathrm{r}}}{m}\left(2\beta - \delta_{\mathrm{r}} - \frac{\gamma l_{\mathrm{r}}}{v}\right),$$

$$E_1 = H_1(\gamma,\psi,v) + G_1(\beta,\gamma,\psi,v) + (F_{\mathrm{fa}}\delta_{\mathrm{f}} + F_{\mathrm{ra}}\delta_{\mathrm{r}})/(mv),$$

$$E_2 = H_2(\gamma,\psi,v,u) + G_2(\beta,\gamma,\psi,v,u) + \frac{l_{\mathrm{f}}F_{\mathrm{fa}}\delta_{\mathrm{f}} - l_{\mathrm{r}}F_{\mathrm{ra}}\delta_{\mathrm{r}}}{I_Z},$$

$$H_1 = \frac{-g\,\sin\alpha\,\cos\psi}{v} + \frac{(-c_{\mathrm{f}}l_{\mathrm{f}} + c_{\mathrm{r}}l_{\mathrm{r}})\,d^2\gamma^3}{mv^4},$$

$$H_2 = \left[-\frac{1}{v}\left(l_{\mathrm{r}}^2c_{\mathrm{r}}v + l_{\mathrm{f}}^2c_{\mathrm{f}}d\gamma\right) - d\left(c_{\mathrm{f}}l_{\mathrm{f}}\delta_{\mathrm{f}} - c_{\mathrm{r}}l_{\mathrm{r}}\delta_{\mathrm{r}}\right)\right]\frac{d\gamma^2}{I_Z v^2},$$

$$G_1 = \left[mg\;\sin\;\alpha\;\sin\psi - \frac{1}{v^2}(c_{\mathrm{f}} + c_{\mathrm{r}})\,d^2\gamma^2\right]\frac{\beta}{mv},$$

$$G_2 = \frac{d\gamma\beta}{v^2I_Z}\left[l_{\mathrm{r}}c_{\mathrm{r}}v - l_{\mathrm{f}}c_{\mathrm{f}}d\gamma - dv\left(\delta_{\mathrm{f}}c_{\mathrm{f}} + \delta_{\mathrm{r}}c_{\mathrm{r}}\right)\right].$$

Additionally, due to the uncertain longitudinal and lateral slips, ε_v, ε_β, and ε_γ are the unknown parts of the vehicle system as follows

$$\varepsilon_v = \Delta F_{v1} + \Delta F_{v2} + \Delta T_a/(Rm),$$

$$\varepsilon_\beta = \Delta A_{11}\beta + \Delta A_{12}\gamma + \Delta B_1[\delta_{\mathrm{f}} \;\; \delta_{\mathrm{r}} \;\; T_{\mathrm{b}}]^{\mathrm{T}} + \Delta H_1 + \Delta G_1,$$

$$\varepsilon_\gamma = \Delta A_{21}\beta + \Delta A_{22}\gamma + \Delta B_2[\delta_{\mathrm{f}} \;\; \delta_{\mathrm{r}} \;\; T_{\mathrm{b}}]^{\mathrm{T}} + d\Delta T_{\mathrm{b}}/(RI_Z), + \Delta H_2 + \Delta G_2 + \Delta C$$

with

$$\Delta C = \frac{d}{I_Z}\Big[(\Delta c_1 - \Delta c_2)\delta_{\mathrm{f}}^2 + (\Delta c_2 - \Delta c_1)\delta_{\mathrm{f}}\beta + (\Delta c_3 - \Delta c_4)\delta_{\mathrm{r}}^2 + (\Delta c_4 - \Delta c_3)\delta_{\mathrm{r}}\beta + \frac{1}{v}(\Delta c_2 - \Delta c_1)l_{\mathrm{f}}\delta_{\mathrm{f}}\gamma + \frac{1}{v}(\Delta c_3 - \Delta c_4)l_{\mathrm{r}}\delta_{\mathrm{r}}\gamma\Big].$$

4) Ideal Reference Model: The controlled off-road vehicle is expected to maintain consistent dynamic properties for drivers, and an ideal reference model of the vehicle running on a horizontal terrain ($\alpha = 0$) is defined as follows

$$\begin{bmatrix} \dot{\beta}_{\mathrm{d}} & \dot{\gamma}_d \end{bmatrix}^{\mathrm{T}} = A\begin{bmatrix} \beta_{\mathrm{d}} & \gamma_{\mathrm{d}} \end{bmatrix}^{\mathrm{T}} + B_{\mathrm{f}}\delta_{\mathrm{f}} \tag{14}$$

where $B_{\mathrm{f}} = [c_{\mathrm{f}}/(mv_{\mathrm{d}}), c_{\mathrm{f}}l_{\mathrm{f}}/I_Z]^{\mathrm{T}}$.

The model (14) is a classic 2-DOF linear bicycle model [34]. Thus, the sideslip angle and the yaw rate of the off-road vehicle running on soft slopes will be controlled to track this ideal reference model.

III. Control System Design

A. Observer for Sideslip Angle

To implement SOSM controllers, the sideslip angle needs to be known. However, the sideslip angle of the vehicle is one of the most difficult parameters to obtain, and is very expensive to use some special sensors to directly measure [35]. Therefore, many topics for the estimation of the sideslip angle have been widely discussed. Extended Kalman filter (EKF) algorithms through a single-track vehicle model could obtain the sideslip angle with low computational burdens [36], [37]. Additionally, Lyapunov-based observers have been proposed for the estimation of the sideslip angle [38], and the gain-scheduling observer can be determined with off-line and on-line computations basing on a linear-parameter-varying (LPV) model of the vehicle [39]. To address model nonlinearities and uncertain slips, a Lyapunov-based SM observer will be designed for estimating the sideslip angle of the vehicle.

An assumption for the vehicle system is given as the following.

Assumption 1: The states and the inputs of system (13) are bounded (BIBS), and there exist some positive constants $\bar{\beta}$, $\bar{\gamma}$, $\underline{v}$, $\bar{v}$, δ_S, and F_S, such that

1) $|\beta| \le \bar{\beta}$, $|\gamma| \le \bar{\gamma}$, $\underline{v} \le v \le \bar{v}$, $|\delta_{\mathrm{f}}| \le \bar{\delta}_{\mathrm{S}}$, and $|\delta_{\mathrm{r}}| \le \bar{\delta}_{\mathrm{S}}$;
2) $|F_{1x}|$, $|F_{2x}|$, $|F_{3x}|$, and $|F_{4x}|$ are all bounded by $F_{\mathrm{S}}/2$.

Remark 1: Owing to physical limits of steering mechanisms and driving motors, the steering angles and the tractions are all bounded. Actually, the steering angles are always much smaller than their physical limits when the vehicle runs at a high speed.

Remark 2: To avoid frequently switching between the driver commands of the brake or accelerator pedal and the inputs of the velocity controller at a low speed, the vehicle speed is assumed to have a lower bound when the velocity controller is effective. Due to safety concerns, the vehicle has a maximum velocity. Thus, the velocity bounded by $\underline{v}$ and $\bar{v}$ is considered in this study, which is 30 km/h $\le v \le$ 80 km/h.

Remark 3: When small front-wheel-steering angles are inputted to the vehicle system (13) by drivers, the sideslip angle is always bounded. In this study, the proposed controllers are designed to follow the ideal model (14) which is under the condition of horizontal terrains ($\alpha = 0$), and to provide consistent steering properties for drivers. Moreover, in some worst-cases scenarios, other controllers [40], [41] could be considered to construct under the layer of the proposed controllers to stabilize lateral dynamics of the vehicle.

Authorized licensed use limited to: Seoul National University. Downloaded on August 26,2024 at 05:27:08 UTC from IEEE Xplore. Restrictions apply.

The following variables are introduced: $x = [\beta,\ \gamma]^{\mathrm{T}}$, $y = [\gamma,\ a_y]^{\mathrm{T}}$, $u = [\delta_{\mathrm{f}},\ \delta_{\mathrm{r}},\ T_{\mathrm{b}}]^{\mathrm{T}}$. Additionally, F_{fa} and F_{ra} are treated as unknown variables. Then, the sideslip angle and the yaw rate in the vehicle model (13) can be recast as

$$\begin{cases} \dot{x}_1 = A_{11}x_1 + A_{12}x_2 + B_1u + H_1 + G_1 + \varepsilon_1 \\ \dot{x}_2 = A_{21}x_1 + A_{22}x_2 + B_2u + H_2 + G_2 + \varepsilon_2 \end{cases} \tag{15}$$

where $\varepsilon_1 = \varepsilon_\beta + \frac{F_{\mathrm{fa}}\delta_{\mathrm{f}} + F_{\mathrm{ra}}\delta_{\mathrm{r}}}{mv}$, $\varepsilon_2 = \varepsilon_\gamma + \frac{l_{\mathrm{f}}F_{\mathrm{fa}}\delta_{\mathrm{f}} - l_{\mathrm{r}}F_{\mathrm{ra}}\delta_{\mathrm{r}}}{I_Z}$.

Remark 4: H_1, G_1, H_2, and G_2 are known functions of states and inputs, and ε_1 and ε_2 are unknown variables in the plant (15). The functions of H_1 and H_2 only include measureable variables x_2, u, ψ and v. Meanwhile, the functions of G_1 and G_2 include the unknown variable x_1 to be estimated.

Under the conditions of Assumption 1, ΔH_1, ΔH_2, ΔG_1, and ΔG_2 are all bounded by some positive constants, which can be calculated as follows

$$\Delta H_1 \le \frac{c_{\mathrm{S}}d\left(l_{\mathrm{f}} + l_{\mathrm{r}}\right)\bar{\gamma}^2}{m\underline{v}^2\left(\underline{v} - d\bar{\gamma}\right)}, \quad \Delta G_1 \le \frac{2c_{\mathrm{S}}d\bar{\gamma}\bar{\beta}}{m\underline{v}\left(\underline{v} - d\bar{\gamma}\right)},$$

$$\Delta H_2 \le \frac{c_{\mathrm{S}}d\bar{\gamma}^2\left[l_{\mathrm{f}}^2 + l_{\mathrm{r}}^2 + \delta_{\mathrm{S}}d\left(l_{\mathrm{f}} + l_{\mathrm{r}}\right)\right]}{\underline{v}I_Z\left(\underline{v} - d\bar{\gamma}\right)},$$

$$\Delta G_2 \le \frac{c_{\mathrm{S}}d\bar{\gamma}\bar{\beta}\left(l_{\mathrm{f}} + l_{\mathrm{r}} + 2d\delta_{\mathrm{S}}\right)}{I_Z\left(\underline{v} - d\bar{\gamma}\right)}.$$

Therefore, two positive constants $\bar{\varepsilon}_1$ and $\bar{\varepsilon}_2$ can be found, such that $\varepsilon_1 \le \bar{\varepsilon}_1$ and $\varepsilon_2 \le \bar{\varepsilon}_2$.

To eliminate some unmatched uncertainties for the observer, the lateral acceleration, which can be easily measured by some sensors, is expressed as follows

$$\begin{aligned} a_y &= v\left(\dot{x}_1 + x_2\right) \\ &= vA_{11}x_1 + v\left(A_{12} + 1\right)x_2 + vB_1u + vH_1 + vG_1 + v\varepsilon_1 \end{aligned} \tag{16}$$

To construct the observer for the actual sideslip angle, an assumption for the parameters and variables of the vehicle is given as the following.

Assumption 2: The parameters in matrixes *A* and *B* are all known. Meanwhile, the slope angle of the terrain, the speed, yaw angle, yaw rate and lateral acceleration of the vehicle can be measured by some sensors, and the vehicle is understeered. Then, the bank and grade angles of the vehicle on the soft and slope terrain can be obtained. Furthermore, the parameters and variables in functions of H_1, H_2, G_1, and G_2 are all known except the state variable of the sideslip angle.

The observer for the sideslip angle of the system (15) is constructed as

$$\begin{cases} \dot{\hat{x}}_1 = A_{11}\hat{x}_1 + A_{12}\hat{x}_2 + B_1u + H_1\left(x_2, \psi, v\right) + \left(a_y - \hat{a}_y\right)/v \\ \qquad\quad + k_1\left(x_2 - \hat{x}_2\right) \\ \dot{\hat{x}}_2 = A_{21}\hat{x}_1 + A_{22}x_2 + B_2u + H_2\left(x_2, u, v\right) + \upsilon \\ \hat{a}_y = vA_{11}\hat{x}_1 + v\left(A_{12} + 1\right)x_2 + vB_1u + vH_1\left(x_2, \psi, v\right) \end{cases} \tag{17}$$

where $\hat{x}_1$ and $\hat{x}_2$ are the estimates of β and γ, respectively; $\hat{a}_y$ is the estimate of a_y; υ and k_1 are the control variables to be designed.

Then, the following conclusion for estimating the sideslip angle of the vehicle is ready to be presented.

Proposition 1: If the observer is designed as (17), the control variable is given as

$$k_1 = -1 + \left(c_{\mathrm{r}}l_{\mathrm{r}} - c_{\mathrm{f}}l_{\mathrm{f}}\right)\left(1/\left(mv^2\right) + 1/I_Z\right) \tag{18}$$

and the control law is give as

$$\upsilon = k_2\mathrm{sign}\left(x_2 - \hat{x}_2\right) \tag{19}$$

with

$$k_2 > \bar{G}_2 + \bar{\varepsilon}_2 \tag{20}$$

then the estimated values $\hat{x}_1$ and $\hat{x}_2$ will track their actual values x_1 and x_2 asymptotically.

Proof: Let $\tilde{x}_1 = x_1 - \hat{x}_1$ and $\tilde{x}_2 = x_2 - \hat{x}_2$. Then, the time derivative of $\tilde{x}_1$ and $\tilde{x}_2$ can be obtained as

$$\begin{cases} \dot{\tilde{x}}_1 = \left(A_{12} - k_1\right)\tilde{x}_2 \\ \dot{\tilde{x}}_2 = A_{21}\tilde{x}_1 + G_2\left(\hat{x}, v, u\right) + \varepsilon_2 - \upsilon \end{cases} \tag{21}$$

Select a Lyapunov function as $V(\tilde{x}_1, \tilde{x}_2) = \tilde{x}_1^2/2 + \tilde{x}_2^2/2$. Taking the derivative of $V(\tilde{x}_1, \tilde{x}_2)$ along (21) yields

$$\begin{aligned} \dot{V} &= \left(A_{12} - k_1\right)\tilde{x}_1\tilde{x}_2 + \tilde{x}_2\left(A_{21}\tilde{x}_1 + G_2\left(\hat{x}, v, u\right) + \varepsilon_2 - \upsilon\right) \\ &= \left(A_{12} + A_{21} - k_1\right)\tilde{x}_1\tilde{x}_2 + \tilde{x}_2\left(G_2\left(\hat{x}, v, u\right) + \varepsilon_2 - \upsilon\right) \end{aligned} \tag{22}$$

Under Assumption 1, there exist a positive constant $\bar{G}_2$ such that $|G_2| \le \bar{G}_2$. Then, applying (18) and (19) into (22) yields

$$\begin{aligned} \dot{V} &\le \tilde{x}_2\left(G_2\left(\hat{x}, v, u\right) + \varepsilon_2 - k_2\mathrm{sign}\left(\tilde{x}_2\right)\right) \\ &\le \left|\tilde{x}_2\right|\left|G_2\left(\hat{x}, v, u\right) + \varepsilon_2\right| - k_2\left|\tilde{x}_2\right| \\ &\le \left|\tilde{x}_2\right|\left(\bar{G}_2 + \bar{\varepsilon}_2 - k_2\right) \end{aligned} \tag{23}$$

It can be inferred from (23) that $\dot{V} < 0$ when $\tilde{x}_2 \ne 0$. According to the Lyapunov and Lasalle invariant set theorems, it is clear that the system (21) can be asymptotically stabilized by the controller, and estimated errors asymptotically converge to zero. Thus, the observer (17) for the sideslip angle of the vehicle will track its real value asymptotically. Thereby, the proof is completed. ■

B. Velocity Controller

To cruise at a constant speed on soft and slope terrains using a velocity controller, the driver will only deploy steering commands to the front wheels without any brake or accelerator pedal input. Meanwhile, stability controllers will be designed to maintain consistent steering properties with the ideal vehicle travelling on a horizontal terrain ($\alpha = 0$). Therefore, to 4WS and 4WID vehicles, the inputs of the proposed controllers for the vehicle system include the total torque, the differential torque, and the rear-wheel-steering angle. Additionally, a torque allocation controller is proposed to exert the torque on each

Authorized licensed use limited to: Seoul National University. Downloaded on August 26,2024 at 05:27:08 UTC from IEEE Xplore. Restrictions apply.

wheel and simultaneously satisfy the results of the total torque and the differential torque.

To the velocity of the vehicle, the first equation of (13) can be rewritten as

$$\dot{v} = F_{v1} - g\sin\alpha\left(\beta\cos\psi + \sin\psi\right) + \frac{1}{mR}T_{\mathrm{a}} + \varepsilon_3 \tag{24}$$

where $\varepsilon_3 = F_{v2} + \varepsilon_v$.

Under Assumption 1, the upper bound of ε_3 can be found as

$$|\varepsilon_3| \le \frac{c_S}{m}\left(\delta_{\mathrm{S}} + \bar{\beta}\right)\left(2\delta_{\mathrm{S}} + 2\bar{\beta} + \frac{l_{\mathrm{f}} + l_{\mathrm{r}}}{\underline{v}}\bar{\gamma}\right) + \frac{c_{\mathrm{r}}\delta_{\mathrm{S}}}{m}\left(2\bar{\beta} + \frac{l_{\mathrm{r}}}{\underline{v}}\bar{\gamma} + \delta_{\mathrm{S}}\right) + \frac{4T_{\mathrm{S}}}{mR} \tag{25}$$

Unlike the virtual actuator in the observer, the chattering phenomenon is harmful to control systems. In fact, SOSM techniques can be used to reduce the chattering problem. To cruise at a stable velocity v_{d}, a SOSM-based ST controller is chosen as follows.

Proposition 2: If the SOSM controller is designed as

$$T_{\mathrm{a}} = \varsigma_1 + \varsigma_2 \tag{26}$$

where

$$\varsigma_1 = mgR\sin\alpha\left(\hat{\beta}\cos\psi + \sin\psi\right) - R\left[c_{\mathrm{f}}\delta_{\mathrm{f}}\left(2\hat{\beta} + \frac{l_f}{v}\gamma - \delta_{\mathrm{f}}\right) - \left(c_{\mathrm{f}} + c_{\mathrm{r}}\right)\hat{\beta}^2 + \hat{\beta}\gamma\frac{c_{\mathrm{f}}l_{\mathrm{f}} - c_{\mathrm{r}}l_{\mathrm{r}}}{v}\right] \tag{27}$$

$$\varsigma_2 = -\lambda_v|v - v_{\mathrm{d}}|^{\frac{1}{2}}\mathrm{sign}\left(v - v_{\mathrm{d}}\right) + \varsigma_3 \tag{28}$$

$$\dot{\varsigma}_3 = \begin{cases} -\varsigma_2 & |\varsigma_2| > \varsigma_{\mathrm{M}} \\ -\alpha_v\mathrm{sign}\left(v - v_{\mathrm{d}}\right) & |\varsigma_2| \le \varsigma_{\mathrm{M}} \end{cases} \tag{29}$$

with

$$\alpha_v > \bar{\varepsilon}_{3c}mR, 0 < q_v < 1, \varsigma_{\mathrm{M}} > \bar{\varepsilon}_3 mR/q_v,$$
$$\lambda > \frac{\left(\alpha_v + mR\bar{\varepsilon}_{3c}\right)\left(1 + q_v\right)}{\left(1 - q_v\right)}\sqrt{\frac{2mR}{\alpha_v - mR\bar{\varepsilon}_{3c}}},$$

then the vehicle will approach the stable velocity v_{d} in a finite time when $|\varepsilon_3| \le \bar{\varepsilon}_3$ and $|\dot{\varepsilon}_3| \le \bar{\varepsilon}_{3c}$.

Proof: The variables δ_{f}, γ, and ψ can be obtained by some sensors under the conditions of Assumption 2, and $\hat{\beta}$ can be estimated by the observer constructed in Proposition 1. Taking time derivative of ε_3 yields

$$\dot{\varepsilon}_3 = \frac{c_{\mathrm{r}}}{m}\dot{\delta}_{\mathrm{r}}\left(2\beta - \frac{l_{\mathrm{r}}}{v}\gamma - \delta_{\mathrm{r}}\right) + \frac{c_{\mathrm{r}}}{m}\dot{\delta}_{\mathrm{r}}\left(2\dot{\beta} - \frac{l_{\mathrm{r}}}{v}\dot{\gamma} + \frac{l_{\mathrm{r}}}{v^2}\dot{v}\gamma - \dot{\delta}_{\mathrm{r}}\right) + \dot{\varepsilon}_v \tag{30}$$

Under the conditions of Assumption 1, terms given in (30) are bounded. Therefore, we can find a positive constant $\bar{\varepsilon}_{3c}$ such that $|\dot{\varepsilon}_3| \le \bar{\varepsilon}_{3c}$.

Choose $e_v = v - v_{\mathrm{d}}$ as the SM surface, and $\dot{v}_{\mathbf{d}} = 0$. Applying (27) into system (24) leads to

$$\dot{e}_v = \varepsilon_3 + \frac{1}{mR}\varsigma_2 \tag{31}$$

Then, according to the theorem of ST algorithms [26], ς_2 and ς_3 can be obtained as shown in (28) and (29). Therefore, it can be concluded that the sliding variable e_v will be stabilized to the origin in a finite time under the controller (26). ■

C. Conventional Yaw Moment Controller

To the conventional yaw moment control without features of rear-wheel steering, the controller is proposed to include inputs of differential tractions. Thus, a SM surface σ_μ is chosen as

$$\sigma_\mu = \gamma - \gamma_{\mathrm{d}} + \mu_\beta\left(\beta - \beta_{\mathrm{d}}\right) \tag{32}$$

where μ_β is a weight coefficient for reflecting the proportion of the sideslip angle.

Then, the SOSM controller with the SM surface of (32) is able to be presented as follows.

Proposition 3: If the SOSM controller for the differential torque is designed as

$$T_{\mathrm{b}} = \xi_1 + \xi_2 \tag{33}$$

where

$$\xi_1 = -\frac{1}{B_{23}}\left[\mu_\beta F_1 + F_2 + \left(\mu_\beta A_{11} + A_{21}\right)\left(\beta - \beta_{\mathrm{d}}\right) + \left(\mu_\beta A_{12} + A_{22}\right)\left(\gamma - \gamma_{\mathrm{d}}\right)\right] \tag{34}$$

$$\xi_2 = -\lambda_\mu|\sigma_\mu|^{1/2}\mathrm{sign}\left(\sigma_\mu\right) + \xi_3 \tag{35}$$

$$\dot{\xi}_3 = \begin{cases} -\xi_2 & |\xi_2| > \mu_{\mathrm{M}} \\ -\alpha_\mu\mathrm{sign}\left(\sigma_\mu\right) & |\xi_2| \le \mu_{\mathrm{M}} \end{cases} \tag{36}$$

then the sliding variable σ_μ can be stabilized to the origin in a finite time by choosing proper α_μ, μ_{M}, q_μ, and λ_μ.

Proof: The proof is omitted for brevity since it is actually similar to the proof of Proposition 2. ■

D. Composite Controllers

With the consideration of longitudinal slips and gravity component effects, the velocity controller in Proposition 2 can maintain the stable velocity v_{d}. To the lateral sideslip of the vehicle, composite controllers are proposed to track the ideal reference model (14). Under the controller in Proposition 2, the model for the sideslip angle and the yaw rate in (13) can be rewritten as

$$\begin{cases} \dot{\hat{\beta}} = A_{11}\hat{\beta} + A_{12}\gamma + B_{11}\delta_{\mathrm{f}} + F_1\left(\hat{\beta}, \gamma, \psi\right) + B_{12}\delta_{\mathrm{r}} + \varepsilon_1 \\ \dot{\gamma} = A_{21}\hat{\beta} + A_{22}\gamma + B_{21}\delta_{\mathrm{f}} + F_2\left(\hat{\beta}, \gamma, \delta_{\mathrm{f}}\right) \\ \qquad + \left(B_{22} + B_{\mathrm{a}}\left(\hat{\beta}, \gamma\right)\right)\delta_{\mathrm{r}} + B_{23}T_{\mathrm{b}} + \varepsilon_2 \end{cases} \tag{37}$$

Authorized licensed use limited to: Seoul National University. Downloaded on August 26,2024 at 05:27:08 UTC from IEEE Xplore. Restrictions apply.

where,

$$F_1 = H_1(\gamma, \psi, v_{\rm d}) + G_1\left(\hat{\beta}, \gamma, v_{\rm d}\right),$$

$$B_a = \frac{d^2 c_{\rm r}\gamma\left(l_{\rm r}\gamma - v_{\rm d}\hat{\beta}\right)}{I_Z\left(v_{\rm d}^2 - d^2\gamma^2\right)},$$

$$F_2 = \left[\frac{-d\left(l_{\rm r}^2 c_{\rm r} v_{\rm d} + l_{\rm f}^2 c_{\rm f} d\gamma\right)}{v_{\rm d} I_Z\left(v_{\rm d}^2 - d^2\gamma^2\right)} + \frac{-d^2 c_{\rm f} l_{\rm f}\delta_{\rm f}}{I_Z\left(v_{\rm d}^2 - d^2\gamma^2\right)}\right]\gamma^2 + \frac{d\gamma\hat{\beta}\left(l_{\rm r}c_{\rm r}v_{\rm d} - l_{\rm f}c_{\rm f}d\gamma - dc_{\rm f}v_{\rm d}\delta_{\rm f}\right)}{I_Z\left(v_{\rm d}^2 - d^2\gamma^2\right)}$$

Additionally, choose a composite disturbance variable as

$$\varepsilon_e = \varepsilon_2 - \left(B_{22} + B_{\mathbf{a}}\right)\varepsilon_1 / B_{12} \tag{38}$$

Then, the composite controllers are ready to be presented.

Proposition 4:

1) If the SOSM controller for the rear-wheel-steering angle is designed as

$$\delta_{\mathbf{r}} = \zeta_1 + \zeta_2 \tag{39}$$

where

$$\zeta_1 = -\frac{1}{B_{12}}\left[A_{11}\left(\hat{\beta} - \beta_{\mathbf{d}}\right) + A_{12}\left(\gamma - \gamma_{\rm d}\right) + F_1\right] \tag{40}$$

$$\zeta_2 = -\lambda_\beta\left|\hat{\beta} - \beta_d\right|^{1/2}\text{sign}\left(\hat{\beta} - \beta_d\right) + \zeta_3 \tag{41}$$

$$\dot{\zeta}_3 = \begin{cases} -\zeta_2 & |\zeta_2| > \zeta_{\rm M} \\ -\alpha_\beta \text{sign}\left(\hat{\beta} - \beta_{\rm d}\right) & |\zeta_2| \le \zeta_{\rm M} \end{cases} \tag{42}$$

with

$$\alpha_\beta > \frac{\bar{\varepsilon}_{1c}}{B_{12}}, 0 < q_\beta < 1, \zeta_{\rm M} > \frac{\bar{\varepsilon}_1}{q_\beta B_{12}},$$

$$\lambda_\beta > \sqrt{\frac{2}{B_{12}\alpha_\beta - \bar{\varepsilon}_{1c}}}\frac{\left(B_{12}\alpha_\beta + \bar{\varepsilon}_{1c}\right)\left(1 + q_\beta\right)}{B_{12}\left(1 - q_\beta\right)},$$

then the sideslip angle of the vehicle will approach $\beta_{\rm b}$ in a finite time when $|\varepsilon_1| \le \bar{\varepsilon}_1$ and $|\dot{\varepsilon}_1| \le \bar{\varepsilon}_{1c}$.

2) If the SOSM controller for the differential torque is designed as

$$T_{\mathbf{b}} = \xi_1 + \xi_2 \tag{43}$$

where

$$\xi_1 = \frac{1}{B_{23}}\left[-\left(A_{22} - \frac{B_{22} + B_{\rm a}}{B_{12}}A_{12}\right)\left(\gamma - \gamma_{\rm d}\right) - F_2 + \frac{B_{22} + B_{\rm a}}{B_{12}}F_1\right] \tag{44}$$

$$\xi_2 = -\lambda_\gamma|\gamma - \gamma_{\rm d}|^{\frac{1}{2}}\ \text{sign}\ \left(\gamma - \gamma_{\rm d}\right) + \xi_3 \tag{45}$$

$$\dot{\xi}_3 = \begin{cases} -\xi_2 & |\xi_2| > \xi_{\rm M} \\ -\alpha_\gamma\ \mathbf{sign}\ \left(\gamma - \gamma_{\rm d}\right) & |\xi_2| \le \xi_{\rm M} \end{cases} \tag{46}$$

with

$$\alpha_\gamma > \frac{\bar{\varepsilon}_{ec}}{B_{23}}, 0 < q_\gamma < 1, \xi_{\rm M} > \frac{\bar{\varepsilon}_e}{q_\gamma B_{23}},$$

$$\lambda_\gamma > \sqrt{\frac{2}{B_{23}\alpha_\gamma - \bar{\varepsilon}_{ec}}}\frac{\left(B_{23}\alpha_\gamma + \bar{\varepsilon}_{ec}\right)\left(1 + q_\gamma\right)}{B_{23}\left(1 - q_\gamma\right)},$$

then the yaw rate of the vehicle will approach $\gamma_{\rm d}$ in a finite time when $|\varepsilon_e| \le \bar{\varepsilon}_e$ and $|\dot{\varepsilon}_e| \le \bar{\varepsilon}_{ec}$.

By using the composite controllers in (39) and (43), the sideslip angle and the yaw rate will track the ideal reference model (14) in a finite time.

Proof: Let $e_1 = \hat{\beta} - \beta_{\mathbf{d}}$, $e_2 = \gamma - \gamma_{\rm d}$, and the time derivative of e_1 and e_2 can be obtained by using the ideal reference system (14) and the plant (37) as

$$\begin{cases} \dot{e}_1 = A_{11}e_1 + A_{12}e_2 + F_1 + B_{12}\delta_{\rm r} + \varepsilon_1 \\ \dot{e}_2 = A_{21}e_1 + A_{22}e_2 + F_2 + \left(B_{22} + B_{\rm a}\right)\delta_{\rm r} + B_{23}T_{\rm b} + \varepsilon_2 \end{cases} \tag{47}$$

Step 1: Choose e_1 as the first SM surface, and the controller for the rear-wheel-steering angle is constructed as (39). Applying (40) into the first equation of (47) gives

$$\dot{e}_1 = \varepsilon_1 + B_{12}\zeta_2 \tag{48}$$

A positive constant $\bar{\varepsilon}_{1c}$ can always be found such that $|\dot{\varepsilon}_1| \le \bar{\varepsilon}_{1c}$ when $\underline{v} \le v \le \bar{v}$. Moreover, based on the condition given in Assumption 1, ε_1 is bounded by $\bar{\varepsilon}_1$. Then, according to the theorem of ST algorithms, the SOSM controller for ζ_2 and ζ_3 can be designed as (41) and (42). Therefore, it can be concluded that the sliding variable e_1 will be stabilized to the origin in a finite time with the controller (39).

Step 2: Under the controller (39), e_1 is limited to and moving on the SM surface

$$e_1 = 0, \quad \dot{e}_1 = 0 \tag{49}$$

Then, on the SM surface of (49), it implies

$$\begin{cases} 0 = A_{12}e_2 + F_1 + B_{12}\delta_{\rm req} + \varepsilon_1 \\ \dot{e}_2 = A_{22}e_2 + F_2 + \left(B_{22} + B_{\rm a}\right)\delta_{\rm req} + B_{23}T_{\rm b} + \varepsilon_2 \end{cases} \tag{50}$$

According to the first equation of (50), the equivalent control $\delta_{\rm req}$ for the SM surface e_1 can be established as

$$\delta_{\rm req} = -\left(A_{12}e_2 + F_1 + \varepsilon_1\right)/B_{12} \tag{51}$$

Substituting the equivalent control $\delta_{\rm req}$ into the second equation of (50) leads to

$$\dot{e}_2 = \left[A_{22} - A_{12}\left(B_{22} + B_{\rm a}\right)/B_{12}\right]e_2 + F_2 - F_1\left(B_{22} + B_{\rm a}\right)/B_{12} + B_{23}T_{\rm b} + \varepsilon_2 - \left[\left(B_{22} + B_{\rm a}\right)/B_{12}\right]\varepsilon_1 \tag{52}$$

Applying (38) and (44) into (52) leads to

$$\dot{e}_2 = \varepsilon_e + B_{23}\xi_2 \tag{53}$$

Authorized licensed use limited to: Seoul National University. Downloaded on August 26,2024 at 05:27:08 UTC from IEEE Xplore. Restrictions apply.

Under Assumption 1, there exists a positive constant $\bar{\varepsilon}_e$ such that $|\varepsilon_e| \leq \bar{\varepsilon}_e$. Taking derivative of ε_e yields

$$\dot{\varepsilon}_e = \dot{\varepsilon}_2 - \left[\left(B_{22} + B_{\mathrm{a}}\right)/B_{12}\right]\dot{\varepsilon}_1 - \dot{B}_{\mathrm{a}}\varepsilon_1/B_{12} \tag{54}$$

The items given in (54) are bounded, and there exists a positive constant $\bar{\varepsilon}_{ec}$ such that $|\dot{\varepsilon}_e| \leq \bar{\varepsilon}_{ec}$. Then, according to the theorem of ST algorithms, the SOSM controller for ξ_2 and ξ_3 can be designed as (45) and (46). Therefore, it can be concluded that the SM variable e_2 will be stabilized to the origin in a finite time by using the controller (43). Finally, by combining controllers (39) and (43), the plant (37) will approach the ideal reference model (14) in a finite time. ■

E. Torque Allocation

As a matter of fact, the 4WID vehicle is an over-actuated system with four independent driving motors, and only two controlled variables with respect to the total torque and the differential torque have been used. Thus, the controllers for vehicle motions are proposed to have the following two layers: the upper layer, which is used to calculate the total torque T_{a} and the differential torque T_{b}, and the lower layer, which is used to optimally allocate the torques to the four motors and simultaneously satisfies the results from the upper layer. By using the velocity controller and the composite controllers, the control inputs of T_{a} and T_{b} have been obtained, and the following functions with respect to the torque of each wheel can be given

$$\underbrace{\begin{bmatrix} T_{\mathrm{A}} \\ T_{\mathrm{B}} \end{bmatrix}}_{u_{\mathbf{d}}} = \underbrace{\begin{bmatrix} 1 & 1 & 1 & 1 \\ -1 & 1 & -1 & 1 \end{bmatrix}}_{B_{\mathrm{L}}} \underbrace{\begin{bmatrix} T_1 \\ T_2 \\ T_3 \\ T_4 \end{bmatrix}}_{u_{\mathrm{L}}} \tag{55}$$

It implies an issue of multiple solutions in (55). In the lower layer, the optimal allocation controller is proposed to minimize the control efforts for the four motors. Then, the cost function J is defined as follows

$$J = \sum_{i=1}^{4} T_i^2 = u_{\mathrm{L}}^{\mathrm{T}} u_{\mathrm{L}} \tag{56}$$

Therefore, the proposed allocation controller is designed to minimize J subject to (55). A Lagrange function is constructed as follows

$$L\left(u_{\mathbf{L}}, \lambda\right) = J + \lambda^{\mathrm{T}}\left(B_{\mathrm{L}} u_{\mathrm{L}} - u_{\mathrm{d}}\right) \tag{57}$$

where $\lambda = [\lambda_1, \lambda_2]^{\mathrm{T}}$ is a Lagrange multiplier. According to least-square solution methods, the optimization problem of the torque allocation for four wheels has been reformulated to solve the saddle point of the Lagrange function (57), and the optimality conditions can be obtained as

$$\begin{cases} 2u_{\mathrm{L}}^{*} + B_{\mathrm{L}}^{\mathrm{T}}\lambda^{*} = 0 \\ B_L u_{\mathrm{L}}^{*} - u_d = 0 \end{cases} \tag{58}$$

where u_{L}^{*} and λ^{*} are the saddle points of $L(u_{\mathrm{L}}, \lambda)$. Since the matrix $B_{\mathrm{L}}B_{\mathrm{L}}^{T}$ is invertible, the optimal torque allocation for the motor of each wheel can be obtained using

$$u_{\mathrm{L}}^{*} = B_{\mathrm{L}}^{T}\left(B_{\mathrm{L}}B_{\mathrm{L}}^{T}\right)^{-1} u_{\mathrm{d}} \tag{59}$$

Therefore, the allocation controller for four motors will exert the torque on each wheel in terms of the torque values given in (59).

TABLE II
MAIN PARAMETERS FOR OFF-ROAD VEHICLE MODEL

Symbol	Value	Symbol	Value
m	720 (kg)	α	10 (°)
l_{f}	1.293 (m)	c_{f}	18100 (N/rad)
l_{r}	1.207 (m)	c_{r}	16700 (N/rad)
d	1.1 (m)	g	9.8 (m/s^2)
R	0.45 (m)	v_{d}	60 (km/h)
I_Z	1090 (kg·m^2)		

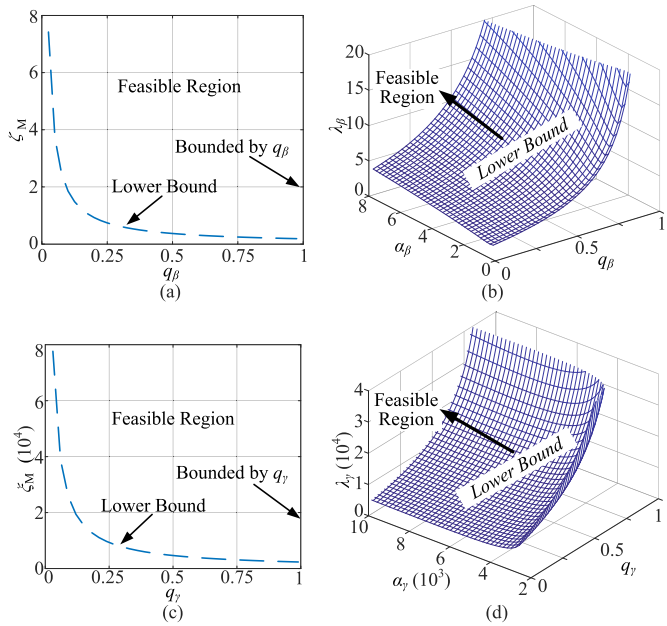

Fig. 2. Feasible regions for parameters of composite controllers. (a) Feasible region for ζ_{M}. (b) Feasible region for λ_β. (c) Feasible region for ξ_{M}. (d) Feasible region for λ_γ.

IV. SIMULATION RESULTS

The values of parameters for the controlled off-road vehicle are shown in Table II.

According to disturbances and uncertainties defined in (13) and (15), the upper bounds of ε_1 and ε_2 are, respectively, set as 0.258 rad/s and 1.780 rad/s^2. Then, for the composite controllers in Proposition 4, feasible regions of α_β and α_γ can be calculated that $\alpha_\beta > 0.1855$ and $\alpha_\gamma > 2330$. Under conditions of $0 < q_\beta < 1$ and $0 < q_\gamma < 1$ in Proposition 4, feasible regions of ζ_{M}, λ_β, ξ_{M} and λ_γ can be calculated as shown in Fig. 2.

The feasible regions for controllers in Propositions 2 and 3 can be similarly calculated. Then, the parameters for the velocity controller (26), the controller (33) only for the differential traction (DT), and the composite controllers (39) and (43) for

Authorized licensed use limited to: Seoul National University. Downloaded on August 26,2024 at 05:27:08 UTC from IEEE Xplore. Restrictions apply.

TABLE III
CONTROL PARAMETERS FOR VEHICLE

Controllers	Parameters
Velocity Controller, (26)	$q_v = 0.1$, $\alpha_v = 1360$, $\varsigma_M = 5895$, $\lambda_v = 1540$.
DT, (33)	$q_\mu = 0.05$, $\mu_\beta = 1$, $\alpha_\mu = 1455$, $\mu_M = 9090$, $\lambda_\mu = 1410$.
DT + RS, (39) and (43)	$q_\beta = 0.05$, $\alpha_\beta = 2.18$, $\zeta_M = 3.8$, $\lambda_\beta = 2.3$; $q_\gamma = 0.05$, $\alpha_\gamma = 4330$, $\xi_M = 4670$, $\lambda_\gamma = 4930$.

the DT and the rear-wheel steering (RS) have been selected as shown in Table III.

For the composite controllers, it can be obtained that $\zeta_M > 3.711$, $\lambda_\beta > 2.2193$, $\xi_M > 4660$, and $\lambda_\gamma > 4916$ when $q_\beta = 0.05, \alpha_\beta = 2.18, q_\gamma = 0.05$, and $\alpha_\gamma = 4330$ are deployed. Therefore, it can be verified that, $\zeta_M = 3.8, \lambda_\beta = 2.3, \xi_M = 4670$ and $\lambda_\gamma = 4930$ are all in their feasible regions for the composite controllers in Proposition 4.

Moreover, the uncertainties ε_1, ε_2 and ε_3 of the system (13) are, respectively, set as $\bar{\varepsilon}_1 \sin(\pi t/5)$, $\bar{\varepsilon}_2 \sin(\pi t/5)$, $\bar{\varepsilon}_3 \sin(\pi t/5)$. In order to analyze the performance of controllers, two maneuvers are considered to implement: 1) straight-line travelling without driver inputs; and 2) steering travelling with driver inputs.

A. Straight-Line Running

When the off-road vehicle moves in a straight line on the soft and slope terrain, the initial position angle of ψ is set as $\pi/4$ ($\psi(0) = \pi/4$), and the driver input for the front-wheel-steering angle is 0 ($\delta_f = 0$). The simulation results are shown in Fig. 3 when the velocity controller, the controller only for DT and the composite controllers for DT and RS are used.

Simulation results in Fig. 3(a) show that the vehicle is able to maintain running at a constant speed by using the velocity controller (26). Meanwhile, the speed of the uncontrolled vehicle decreases rapidly due to the initial value of ψ, which implies the off-road vehicle climbs up the soft and slope terrain. Additionally, it can be seen from Figs. 3(b), (c), and (d) that the composite controllers (39) and (43) are effective in tracking the ideal reference model (14) and following the desired straight-line path. When no steering input from the driver is used, the actual ideal sideslip angle and yaw rate of the vehicle should always be zero, and the trajectory would be a straight line. However, the controller (33) is not able to follow the ideal reference model and maintain the vehicle travelling in a straight-line path.

Simulation results in Fig. 3(e) show that motor torque for four wheels from (39) of the composite controllers are larger than the ones from controller (33). As a matter of fact, the composite controllers need generate more torques for the wheels to compensate the additional reversed yaw moment produced by the steering angle of the rear wheels from (43) as shown in Fig. 3(f). Moreover, due to the continuous property of SOSM control methods, all controllers of (26), (39), (43) and (33) have almost no chattering. Figs. 3(g), (h) and (i) take further analysis of simulation results for the velocity controller (26) and the composite controllers of (39) and (43), and show errors of the velocity, the sideslip angle and the yaw rate for keeping

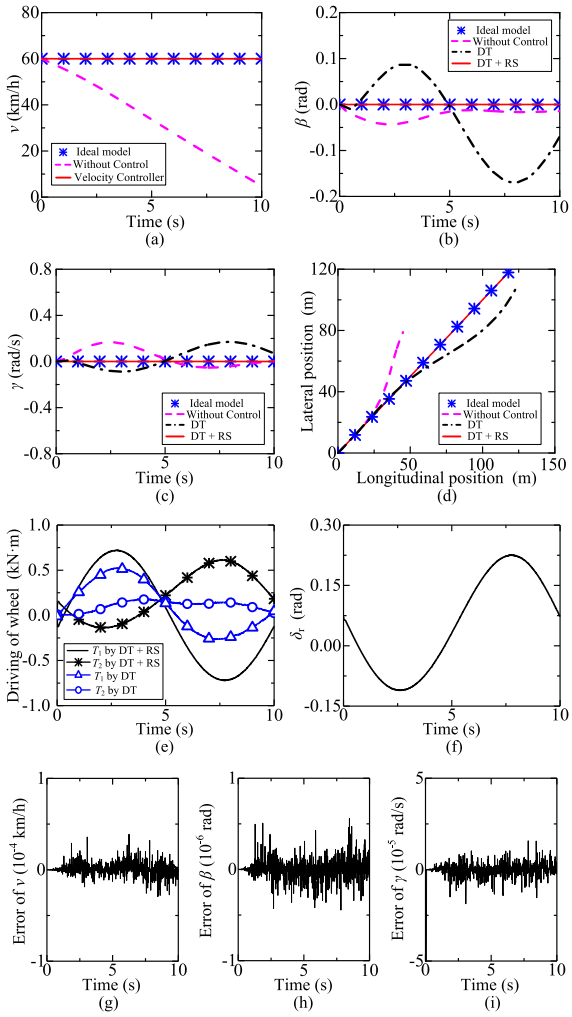

Fig. 3. Simulation results. (a) Velocity. (b) Sideslip angle. (c) Yaw rate. (d) Vehicle trajectory. (e) Torque of wheel. (f) Steering angle of rear wheels. (g) Velocity errors. (h) Sideslip angle errors. (i) Yaw rate errors.

the constant velocity and tracking the ideal reference model. It can be seen that all the errors can be kept at a low level.

B. Steering Running

In simulations of steering running, the driver gives the steering input to front wheels as $0.04\sin(\pi t/5)$, and the initial position angle of ψ is set as 0 ($\psi(0) = 0$). In comparisons with simulation results by using the velocity controller, the controller of only DT, and the composite controllers of DT and RS are shown in Fig. 4.

It is clearly seen from Fig. 4(a) that the vehicle by using the velocity controller (26) can precisely keep the constant velocity when there are some steering inputs from the driver. Meanwhile, the responses of the yaw rate, the sideslip angle, and the trajectory of the vehicle under the composite controllers (39) and (43) are able to accurately approach the ideal reference model (14), as shown in Figs. 4(b), (c), and (d). Moreover, simulation results in Figs. 4(g), (h) and (i) show the high performance of tracking errors. Note that, the yaw rate of the vehicle with the controller

Authorized licensed use limited to: Seoul National University. Downloaded on August 26,2024 at 05:27:08 UTC from IEEE Xplore. Restrictions apply.

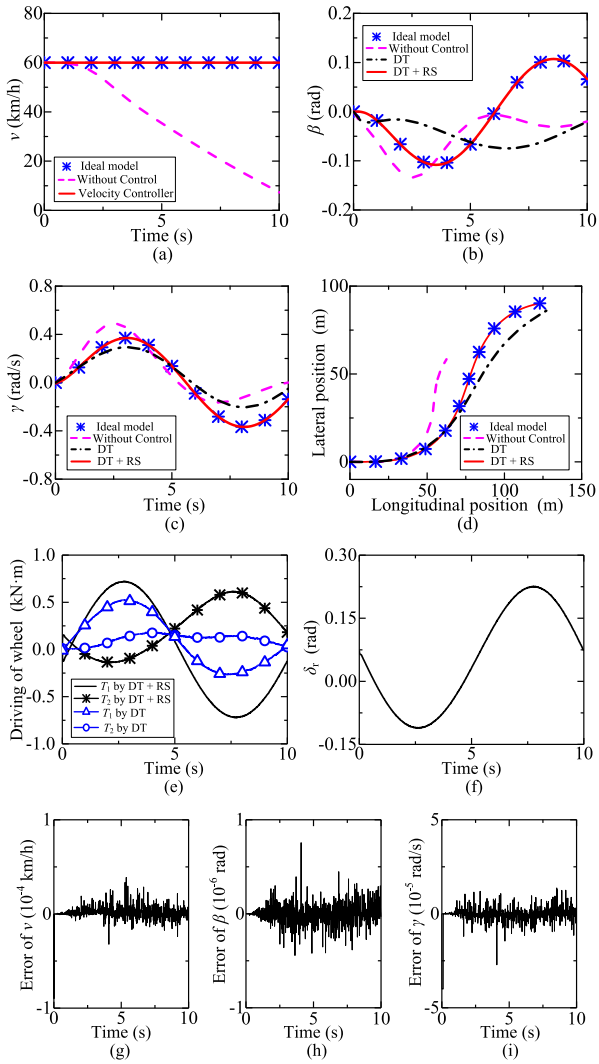

Fig. 4. Simulation results. (a) Velocity. (b) Sideslip angle. (c) Yaw rate. (d) Vehicle trajectory. (e) Torques of wheel. (f) Steering angle of rear wheels. (g) Velocity errors. (h) Sideslip angle errors. (i) Yaw rate errors.

(33) can be kept in a stable region, whereas the sideslip angle is not able to follow the one of the ideal reference model.

Simulation results in Figs. 4(e) and (f) show the torques for four wheels using (39) of the composite controllers are larger than the ones using controller (33), due to the additional yaw moment produced by (43). Furthermore, SOSM control methods for controllers (26), (39)–(43), and (33) show the approximately no chattering of actuators.

V. Conclusion

In this paper, SOSM-based ST algorithms were implemented to stabilize an off-road vehicle running on a soft and slope terrain. Under conditions of uncertain longitudinal and lateral slips, the velocity controller was designed to maintain a stable velocity for the vehicle, and the composite controllers were designed to approach an ideal reference model. On this basis, the steering angle of rear wheels, the total torque, and the differential torque were obtained by using the composite controllers, and the torque allocation controller was designed to exert torque on each wheel. Compared with the conventional yaw moment control without rear-wheel steering, the composite controllers were more effective to follow the yaw rate, the sideslip angle and the trajectory of the ideal reference model, whereas more driving toque had to be implemented on each wheel to compensate the additional yaw moment produced by the rear-wheel steering.

References

[1] J. Choi *et al.*, "Environment-detection-and-mapping algorithm for autonomous driving in rural or off-road environment," *IEEE Trans. Intell. Transp. Syst.*, vol. 13, no. 2, pp. 974–982, Jun. 2012.

[2] P. Freeman, M. Jensen, J. Wagner, and K. Alexander, "A comparison of multiple control strategies for vehicle run-off-road and return," *IEEE Trans. Veh. Technol.*, vol. 64, no. 3, pp. 901–911, Mar. 2015.

[3] M. Acosta, S. Kanarachos, and M. E. Fitzpatrick, "Robust virtual sensing for vehicle agile manoeuvring: A tyre-model-less approach," *IEEE Trans. Veh. Technol.*, vol. 67, no. 3, pp. 1894–1908, Mar. 2018.

[4] G. Ishigami, A. Miwa, K. Nagatani, and K. Yoshida, "Terramechanics-based model for steering maneuver of planetary exploration rovers on loose soil," *J. Field Robot.*, vol. 24, no. 3, pp. 233–250, Mar. 2007.

[5] Z. C. Liang, J. Chen, and Y. F. Wang, "Equivalent acceleration imitation for single wheel of manned lunar rover by varying torque on earth," *IEEE/ASME Trans. Mechatronics*, vol. 25, no. 1, pp. 282–293, Feb. 2020, doi: 10.1109/TMECH.2019.2953330.

[6] M. G. Bekker, *Introduction to Terrain-Vehicle Systems*, Ann Arbor, Michigan, USA: Univ. Michigan Press, 1969.

[7] Z. Janosi, and B. Hanamoto, "Analytical determination of drawbar pull as a function of slip for tracked vehicle in deformable soils." in *Proc. 1st Int. Conf. Int. Soc. Terrain Vech. Syst.*, Torino, Italy, 1961, pp. 707–726.

[8] Z. Z. Jia, W. Smith, and H. Peng, "Terramechanics-based wheel–terrain interaction model and its applications to off-road wheeled mobile robots," *Robotica*, vol. 30, no. 3, pp. 491–503, May 2012.

[9] G. Ishigami, K. Nagatani, and K. Yoshida, "Slope traversal controls for planetary exploration rover on sandy terrain," *J. Field Robot.*, vol. 26, no. 3, pp. 264–286, Mar. 2019.

[10] W. H. Li, L. Ding, H. B. Gao, and M. Tavakoli, "Haptic tele-driving of wheeled mobile robots under nonideal wheel rolling, kinematic control and communication time delay," *IEEE Trans. Syst., Man, Cybern., Syst.*, vol. 50, no. 1, pp. 336–347, Jan. 2020.

[11] J. N. Wang, Z. Luo, Y. Wang, B. Yang, and F. Assadian, "Coordination control of differential drive assist steering and vehicle stability control for four-wheel-independent-drive EV," *IEEE Trans. Veh. Technol.*, vol. 12, no. 67, pp. 11453–11467, Dec. 2018.

[12] Z. Dong, Y. Yu, W. Li, B. Wang, and D. Xu, "Flux-weakening control for induction motor in voltage extension region: Torque analysis and dynamic performance improvement," *IEEE Trans. Ind. Electron.*, vol. 65, no. 5, pp. 3740–3751, May 2018.

[13] S. Ding, L. Liu, and W.X. Zheng, "Sliding mode direct yaw-moment control design for in-wheel electric vehicles," *IEEE Trans. Ind. Electron.*, vol. 64, no. 8, pp. 6752–6762, Aug. 2017.

[14] Q. Wang, B. Ayalew, and T. Weiskircher, Q. Wang, B. Ayalew, and T. Weiskircher, "Predictive maneuver planningfor an autonomous vehicle in public highway traffic," *IEEE Trans. Intell. Transp. Syst.*, vol. 20, no. 4, pp. 1303–1315, Apr. 2019.

[15] P. Falcone, F. Borrelli, J. Asgari, H. E. Tseng, and D. Hrovat, "Predictive active steering control for autonomous vehicle systems," *IEEE Trans. Control Syst. Technol.*, vol. 15, no. 3, pp. 566–580, May 2007.

[16] M. Choi, and S. B. Choi, "Model predictive control for vehicle yaw stability with practical concerns," *IEEE Trans. Veh. Technol.*, vol. 63, no. 8, pp. 3539–3548, Oct. 2014.

[17] S. Cheng, L. Li, M. M. Mei, Y. L. Nie, and L. Zhao, "Multiple-objective adaptive cruise control system integrated with DYC," *IEEE Trans. Veh. Technol.*, vol. 68, no. 5, pp. 4550–4559, May 2019.

[18] J. Ji, A. Khajepour, W. W. Melek, and Y. J. Huang, "Path planning and tracking for vehicle collision avoidance based on model predictive control with multiconstraints," *IEEE Trans. Veh. Technol.*, vol. 66, no. 2, pp. 952–964, Feb. 2017.

[19] S. Di Cairano, D. Bernardini, A. Bemporad, and I. V. Kolmanovsky, "Stochastic MPC with learning for driver-predictive vehicle control and its application to HEV energy management," *IEEE Trans. Control Syst. Technol.*, vol. 22, no. 3, pp. 1018–1031, May 2014.

Authorized licensed use limited to: Seoul National University. Downloaded on August 26,2024 at 05:27:08 UTC from IEEE Xplore. Restrictions apply.

[20] L. Li, Y. S. Lu, R. R. Wang, and J. Chen, "A three-dimensional dynamics control framework of vehicle lateral stability and rollover prevention via active braking with MPC," *IEEE Trans. Ind. Electron.*, vol. 64, no. 4, pp. 3389–3401, Apr. 2017.
[21] J. H. Guo, P. Hu, and R. B. Wang, "Nonlinear coordinated steering and braking control of vision-based autonomous vehicles in emergency obstacle avoidance," *IEEE Trans. Intell. Transp. Syst.*, vol. 17, no. 11, pp. 3230–3240, Nov. 2016.
[22] J. Yang, W. H. Chen, S. Li, L. Guo, and Y. Yan, "Disturbance/uncertainty estimation and attenuation techniques in PMSM drives—A survey," *IEEE Trans. Ind. Electron.*, vol. 64, no. 4, pp. 3273–3285, Apr. 2017.
[23] A. Levant, "Sliding order and sliding accuracy in sliding mode control," *Int. J. Control*, vol. 58, no. 6, pp. 1247–1263, Dec. 1993.
[24] Y. Feng, F. L. Han, and X. H. Yu, "Chattering free full-order sliding-mode control," *Automatica*, vol. 40, no. 4, pp. 1310–1314, Apr. 2014.
[25] W. H. Chen, J. Yang, L. Guo, and S. H. Li, "Disturbance observer-based control and related methods: An overview," *IEEE Trans. Ind. Electron.*, vol. 63, no. 2, pp. 1083–1095, Feb. 2016.
[26] S. Kuntanapreeda, "Super-twisting sliding-mode traction control of vehicles with tractive force observer," *Control Eng. Pract.*, vol. 38, pp. 26–36, May 2015.
[27] J. Pico, E. Pico-Marco, A. Vignoni, and H. De Battista, "Stability preserving maps for finite-time convergence: Super-twisting sliding-mode algorithm," *Automatica*, vol. 49, no. 2, pp. 534–539, Feb. 2013.
[28] C. Hu, R. R. Wang, and F. J. Yan, "Integral sliding mode-based composite nonlinear feedback control for path following of four-wheel independently actuated autonomous vehicles," *IEEE Trans. Transp. Electrific.*, vol. 2, no. 2, pp. 221–230, Jun. 2016.
[29] M. Kazemi, and K. H.Shirazi, "Handling enhancement of a sliding-mode control assisted four-wheel steer vehicle," in *Proc. IMechE. Part D: J. Automobile Eng.*, vol. 226, no. D2, pp. 234–246, 2012.
[30] A. Alfi, and M. Farrokhi, "Hybrid state-feedback sliding-mode controller using fuzzy logic for four-wheel-steering vehicles," *Vehicle Syst. Dyn.*, vol. 47, no. 3, pp. 265–284, 2009.
[31] Z. C. Liang, H. B. Gao, L. Ding, Z. Q. Deng, and J. J. Qu, "Analysis of driving efficiency for LRV wheels using forced-slip method," *Adv. Space Res.*, vol. 54, no. 10, pp. 2122–2130, 2014.
[32] Z. C. Liang, J. Chen, Y. F. Wang, L. Ding, H. B. Gao, and Z. Q. Deng, "Approach for imitation of manned lunar rover acceleration using a prototype vehicle with imitation handling ratio on the earth," *IEEE Trans. Veh. Technol.*, vol. 67, no. 7, pp. 5683–5694, Jul. 2018.
[33] H. B. Gao *et al.*, "Tracking control of WMRs on loose soil based on mixed H-2/H-infinity control with longitudinal slip ratio estimation," *Acta Astronautica*, vol. 140, no. 49–58, Nov. 2017.
[34] Z. C. Liang, H. B. Gao, L. Ding, and Z. Q. Deng, "Approach to imitate maneuvering of lunar roving vehicle under lunar gravity using a terrestrial vehicle," *Mechatronics*, vol. 30, no. 9, pp. 383–398, 2015.
[35] D. M. Bevly, J. Ryu, and J. C. Gerdes, "Integrating INS sensors with GPS measurements for continuous estimation of vehicle sideslip, roll, and tire cornering stiffness," *IEEE Trans. Intell. Transp. Syst.*, vol. 7, no. 4, pp. 483–493, Dec. 2006.
[36] Y. W. Liao and F. Borrelli, "An adaptive approach to real-time estimation of vehicle sideslip, road bank angles, and sensor bias," *IEEE Trans. Veh. Technol.*, vol. 68, no. 8, pp. 7443–7454, Aug. 2019.
[37] K. Nam, H. Fujimoto, and Y. Hori, "Lateral stability control of in-wheel-motor-driven electric vehicles based on sideslip angle estimation using lateral tire force sensors," *IEEE Trans. Veh. Technol.*, vol. 61, no. 5, pp. 1972–1985, Jun. 2012.
[38] E. Hashemi, S. Khosravani, A. Khajepour, A. Kasaiezadeh, S. K. Chen, and B. Litkouhi, "Longitudinal vehicle state estimation using nonlinear and parameter-varying observers," *Mechatronics*, vol. 34, pp. 28–39. May 2017.
[39] H. Zhang, X. Y. Huang, J. M. Wang, and H. R. Karimi, "Robust energy-to-peak sideslip angle estimation with applications to ground vehicles," *Mechatronics*, vol. 30, no. 338–347, pp. 338–347, Sep. 2015.
[40] J. Ahmadi, A. K. Sedigh, and M. Kabganian, "Adaptive vehicle lateral plane motion control using optimal tire friction forces with saturation limits consideration," *IEEE Trans. Veh. Technol.*, vol. 58, no. 8, pp. 4098–4107, Oct. 2009.
[41] H. P. Du, N. Zhang, and G. M. Dong, "Stabilizing vehicle lateral dynamics with considerations of parameter uncertainties and control saturation through robust yaw control," *IEEE Trans. Veh. Technol.*, vol. 59, no. 5, pp. 2593–2597, Jun. 2010.

Zhongchao Liang received the M.S. and Ph.D. degrees in mechanical engineering from the Harbin Institute of Technology, Harbin, China, in 2011 and 2015, respectively.

He is currently an Associate Professor with the School of Mechanical Engineering and Automation, Northeastern University, Shenyang, China. His research interests include intelligent vehicles and mobile robots.

Jing Zhao received the Ph.D. degree in electromechanical engineering from the University of Macau, Macau, China.

He is currently working with the School of Mechanical Engineering and Automation, Northeastern University, Shenyang, China. His research interests include vehicle dynamics and control, mechanism and machine theory, fluid mechanics, and finite element analysis.

Zhen Dong received the B.S. and M.S. degrees in electrical engineering from the Harbin Institute of Technology, Harbin, China, in 2016 and 2018, respectively. He is currently working toward the Ph.D. degree in control systems with the Department of Electrical and Electronic Engineering, the University of Manchester, Manchester, U.K.

His research interests include distributed control of renewable energy integrated power systems and motor drives.

Yongfu Wang received the Ph.D. degree in control science and engineering from Northeastern University, Shenyang, China, in 2005.

He is currently a Professor with the School of Mechanical Engineering and Automation, Northeastern University, Shenyang, China. His research interests include fuzzy control, electric vehicle, and mechatronic systems.

Zhengtao Ding (Senior Member, IEEE) received the B.Eng. degree from Tsinghua University, Beijing, China, the M.Sc. degree in systems and control, and the Ph.D. degree in control systems from the University of Manchester Institute of Science and Technology, Manchester, U.K.

After working as a Lecturer with Ngee Ann Polytechnic, Singapore, for ten years, he joined the University of Manchester in 2003, where he is currently a Professor of Control Systems with the Department of Electrical and Electronic Engineering. He is the author of the book *Nonlinear and Adaptive Control Systems* (IET, 2013) and a number of journal papers. His research interests include nonlinear and adaptive control theory and their applications, more recently network-based control, distributed optimization and distributed machine learning, with applications to power systems and robotics.

Prof. Ding has served as an Associate Editor for the IEEE TRANSACTIONS ON AUTOMATIC CONTROL, IEEE CONTROL SYSTEMS LETTERS, *Journal of Franklin Institute*, and several other journals.

Authorized licensed use limited to: Seoul National University. Downloaded on August 26,2024 at 05:27:08 UTC from IEEE Xplore. Restrictions apply.